Progress In Electromagnetics Research, Vol. 128, 195–214, 2012

CONSTRAINED TRILINEAR DECOMPOSITION WITH APPLICATION TO ARRAY SIGNAL PROCESSING

X. Liu[1, *], T. Jiang[2], L. X. Yang[1], and H. B. Zhu[1]

[1]College of Telecommunications and information Engineering, Nanjing University of Posts & Telecommunications, Jiangsu Key Laboratory of Wireless Communication, Nanjing, China

[2]Nanjing Panda Technology Co., Ltd., Nanjing, China

Abstract—This paper links the constrained trilinear tensor model into array signal processing. The structure properties of baseband signal, such as the Constant-Modulus (CM) and Finite Alphabet (FA) structures which are already known in the receiving array, are exploited in trilinear decomposition. Two novel algorithms for constrained trilinear decomposition are proposed and applied to array signal processing. The distinguishing features of the proposed model and algorithms compared to the traditional trilinear signal processing methods are: (i) the proposed model has a better performance and lower computation complexity. (ii) it can still work well even if degeneracy of factors are involved in the data model, which is not valid in traditional algorithms. Simulation results are presented to illustrate the application of the constrained trilinear decomposition to array signal processing and evaluate the performance of the proposed algorithms in DOAs estimation.

1. INTRODUCTION

In electromagnetics and signal processing area, antenna arrays have been widely applied to locate various types of signals and improve system performance [1]. The main work of array signal processing is the estimation of parameters and signals by utilizing temporal and spatial information from the samples of receive antenna arrays [2–5]. Many effective methods, such as MUSIC, ESPRIT, PCA and HOS, have been developed to deal with direction finding,

Received 14 March 2012, Accepted 15 May 2012, Scheduled 29 May 2012

* Corresponding author: Xu Liu (liuxu@njupt.edu.cn).

polarization estimation, and signal detection [6–8]. Recently, trilinear decomposition has been exploited to be an effective method in array signal processing. Some trilinear models, such as PARAllel FACtor (PARAFAC) and PARAllel profiles with LINear Dependencies (PARALIND), have been applied to parameter estimation, signal detection, etc. [9–11], due to their powerful unique properties which are not shared by vector or matrix models [12]. In array signal processing aspect, trilinear decomposition can be classified as a high-dimension generalization of ESPRIT algorithm and joint approximate diagonalization (JAD) method [13]. Sidiropoulos et al. firstly introduced trilinear analysis to multiple invariance sensor array processing (MI-SAP) [9]. They applied PARAFAC model to estimate the azimuth and elevation angles from different sources in a uniform square array. Beamforming [14, 15], polarization sensitive array processing [16–18] and MIMO radar location [19, 20] have also been linked to trilinear analysis. The common characteristic of tensor modeling approach in these applications is that baseband signals and array response vectors, which are always involved in data model, are treated as pure 'double-precision' or 'complex' data during trilinear decomposition. However, this kind of simplication implies that some superior structure properties of these data, such as constant-modulus (for phase/frequency modulated signal) and Vandermonde structure (for uniform array response), are ignored, which may cause potential performance loss during signal processing.

Trilinear alternating least square (TALS) algorithm is often used to accomplish trilinear decomposition in PARAFAC-based signal processing [21, 22]. Although TALS has some superior properties, such as simplicity formulation and monotone convergence, it still suffers from some inherent problems, for example, low convergence speed, in following cases:

a) High correlated factors involved in trilinear model. This condition is often defined as "presence of degeneracy" and appears when coherent signals are considered [23–25].
b) Initialized by random numbers. Sometimes, random initialization may cause local minimum or low convergent speed in TALS.

Several methods have been proposed to improve the performance of TALS algorithm, some of which are compression [26], line search [27], enhanced line search [28, 29], and optimized initialization [30]. In fluorescence spectroscopy and flow injection analysis, Bro et al. have pointed out that the performance of trilinear decomposition can be improved when the multi-way data have some special structure [31]. As we have mentioned, baseband signals have some structural properties where the receiving end is always aware of. This paper exploits

structural properties of baseband signal in PARAFAC analysis. A constrained PARAFAC model is introduced as a mathematical tool for modeling array signals. Two novel algorithms are proposed for constrained PARAFAC decomposition and then applied to parameter estimation in array signal processing. The distinguishing improvements of the proposed model and algorithms compared to the already existing tensor-based signal processing methods are:

i). The proposed trilinear model exploits the structure of signals to improve the performance of parameter estimation in array signal processing applications. Simulations will give an example that constrained PARAFAC decomposition has better accuracy in parameters estimation than traditional methods.

ii). As an iteration method, the proposed trilinear decomposition algorithm has better convergence performance and lower computation complexity than TALS-based trilinear signal processing method.

iii). The proposed method still has good performance when some factors of model are "degeneracy", which is not valid in the traditional TALS-based method.

The rest of this paper is outlined as follows. Section 2 defines the constrained PARAFAC model. In Section 3, two iterative algorithms are proposed for constrained PARAFAC decomposition. Some related works, such as convergence property, complexity analysis, and initialization methods, are also discussed in this section. In Section 4, we apply constrained trilinear model to array signal processing. Simulations are presented to evaluate the given algorithms in parameter estimation. In the last section, we summarize the conclusion.

Some notation conventions will be used in this paper. $\mathrm{diag}\left([a,\, b\ldots]\right)$ denotes the diagonal matrix with diagonal scalar entries $a, b, \ldots$ while $\mathrm{blockdiag}\left([\mathbf{A},\, \mathbf{B}\ldots]\right)$ denotes the block diagonal matrix with diagonal matrix entries $\mathbf{A}$, $\mathbf{B}$, ... $(\cdot)^T$ and $(\cdot)^\dagger$ stand for transpose and pseudo-inverse, respectively. $||\cdot||_F^2$ stands for Frobenius norm. $\mathrm{vec}\,(\cdot)$ stacks the columns of its matrix argument in a vector. $\mathrm{unvec}\,(\cdot)$ is the inverse operation of $\mathrm{vec}\,(\cdot)$, $\mathrm{unvec}(\mathbf{c}, I, J) = [\mathbf{c}(1:J), \mathbf{c}(J+1:2J), \ldots, \mathbf{c}((I-1)J:IJ)]$. $\otimes$ is Kronecker product. $\odot$ denotes the Khatri-Rao product, which is a column-wise Kronecker product. Define $\mathbf{A} = [\mathbf{a}_1, \ldots, \mathbf{a}_R] \in \mathbb{C}^{I\times R}$, $\mathbf{B} = [\mathbf{b}_1, \ldots, \mathbf{b}_R] \in \mathbb{C}^{J\times R}$. The Khatri-Rao product of $\mathbf{A}$ and $\mathbf{B}$ is:

$$\mathbf{A} \odot \mathbf{B} = [\mathbf{a}_1 \otimes \mathbf{b}_1, \ldots, \mathbf{a}_R \otimes \mathbf{b}_R]$$

2. CONSTRAINED PARAFAC MODEL

In this section, constrained PARAFAC model is formulated as the basic modeling tool in array signal processing. Firstly, we give the basic form of PARAFAC model. Define a three-order tensor $\bar{\mathbf{X}} \in \mathbb{C}^{I\times J\times K}$ with elements of $\bar{x}_{i,j,k}$. $\bar{\mathbf{X}}$ can be represented as a sum of tensor products [30].

$$\bar{\mathbf{X}} = \mathbf{a}_1 \circ \mathbf{b}_1 \circ \mathbf{c}_1 + \ldots + \mathbf{a}_R \circ \mathbf{b}_R \circ \mathbf{c}_R = \sum_{r=1}^{R} \mathbf{a}_r \circ \mathbf{b}_r \circ \mathbf{c}_r \qquad (1)$$

where $\mathbf{a}_r \in \mathbb{C}^{I\times 1}$, $\mathbf{b}_r \in \mathbb{C}^{J\times 1}$, $\mathbf{c}_r \in \mathbb{C}^{K\times 1}$, $r = 1, \ldots, R$ and $\circ$ denotes the outer product of tensors. Figure 1 gives a illustration of (1).

R is defined as the rank of three-order tensor $\bar{\mathbf{X}}$. Assume that $a_{i,r}$, $b_{j,r}$, $c_{k,r}$ are elements of $\mathbf{a}_r$, $\mathbf{b}_r$, $\mathbf{c}_r$. As the scalar form of (1), $x_{i,j,k}$ can be formulated as a sum of triple products.

$$\bar{x}_{i,j,k} = a_{i,1}b_{j,1}c_{k,1} + , \ldots , + a_{i,R}b_{j,R}c_{k,R} = \sum_{r=1}^{R} a_{i,r}b_{j,r}c_{k,r} \qquad (2)$$

Equations (1) and (2) are variably known as PARAFAC model, trilinear decomposition or canonical decomposition [32]. Define three matrices $\mathbf{A} = [\mathbf{a}_1, \ldots, \mathbf{a}_R]$, $\mathbf{B} = [\mathbf{b}_1, \ldots, \mathbf{b}_R]$, $\mathbf{C} = [\mathbf{c}_1, \ldots, \mathbf{c}_R]$. $\mathbf{A}$, $\mathbf{B}$, $\mathbf{C}$ are defined as "mode matrix" of a given PARAFAC model.

When PARAFAC analysis is adopted in array signal processing, the mode matrices represent meaningful physical interpretation and usually have structure properties. Especially, baseband signal matrix is usually one of the mode matrices, for example, in applications of [9, 10, 13]. Modulated signals usually have special structures which are already known in the receiving end. Many works have exploited these structure properties to bilinear decomposition (matrix analysis) for blind signal separation and parameter estimation [33, 34]. However, as we have mentioned, baseband signal is only considered as simple 'data', not a 'signal' in traditional trilinear signal processing. The

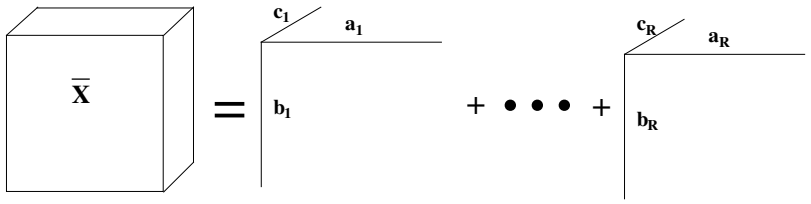

Figure 1. PARAFAC model.

traditional algorithms usually do not hold and utilize these prior structures.

In this study, structure properties are exploited in PARAFAC analysis. Assume that mode matrix $\mathbf{C}$ stands for the signal matrix in (2). The scalar form of the constrained PARAFAC model can be formulated as follow:

$$\bar{x}_{i,j,k} = \sum_{r=1}^{R} a_{i,r} b_{j,r} c_{k,r}, c_{k,r} \in \Omega \tag{3}$$

where Ω denotes a constrained data set. In this paper, Ω stands for FA or CM constraint. By exploiting the structure constraints, model (3) is more appropriate to characterize array signals than traditional trilinear data model. Furthermore, it is shown that the proposed fitting algorithm, which will be given in the next section, can improve the performance in array signal processing applications.

3. ALGORITHMS

In this section, we propose two algorithms, named Trilinear Alternating Least Square with Projection (TALSP) and Trilinear Alternating Least Square with Successive Interference Cancellation (TALSSIC), for constrained PARAFAC decomposition. TALSP algorithm utilizes 'projection' method to reconstruct structure of baseband signals, which can be viewed as a high order extension of FA-based projection method [33]. It has simple formulation and low computation complexity. TALSSIC algorithm exploits 'successive interference cancellation' to reconstruct structure in column wise and is guaranteed to be strictly monotonically convergent during iteration. With a good initialization, TALSSIC algorithm can converge rapidly to the ML estimation.

Before giving the algorithms, we rearrange 3-D tensor to 2-D matrices to simplify algorithm analysis. Consider the formulation of $\bar{\mathbf{X}}$ in the presence of noise

$$\tilde{\mathbf{X}} = \bar{\mathbf{X}} + \bar{\mathbf{E}} \tag{4}$$

where $\bar{\mathbf{E}}$ is Gauss noise triple matrix. Slice $\tilde{\mathbf{X}}$ along three directions and rearrange the elements of $\tilde{\mathbf{X}}$. $\tilde{\mathbf{X}}$ can be formulated into three 'slice' matrices $\mathbf{X}$, $\mathbf{Y}$, $\mathbf{Z}$ [20]

$$\begin{aligned} \mathbf{X}^{IJ\times K} &= (\mathbf{A} \odot \mathbf{B})\, \mathbf{C}^T + \mathbf{E}_X \\ \mathbf{Y}^{JK\times I} &= (\mathbf{B} \odot \mathbf{C})\, \mathbf{A}^T + \mathbf{E}_Y \\ \mathbf{Z}^{KI\times J} &= (\mathbf{C} \odot \mathbf{A})\, \mathbf{B}^T + \mathbf{E}_Z \end{aligned} \tag{5}$$

where $[\mathbf{X}]_{(i-1)J+j,k} = [\mathbf{Y}]_{(j-1)K+k,i} = [\mathbf{Z}]_{(k-1)I+i,j} = \bar{x}_{i,j,k}$. $\mathbf{E}_{X,Y,Z}$ are three Gauss noise slice matrices. The cost function of matrix variables $\mathbf{A}$, $\mathbf{B}$ and $\mathbf{C}$ is defined as:

$$f(\mathbf{A}, \mathbf{B}, \mathbf{C}; \mathbf{X}) = \left|\left|\mathbf{X} - (\mathbf{A} \odot \mathbf{B})\, \mathbf{C}^T\right|\right|_F^2 \tag{6}$$

3.1. TALSP Algorithm

TALSP is a kind of alternating iteration algorithm. Let $(\cdot)^{(k)}$ stand for the value obtained in the k-th iteration. There are two steps in the k-th update procedure of matrix $\mathbf{C}$.

First step: given estimation $\hat{\mathbf{A}}^{(k-1)}$, $\hat{\mathbf{B}}^{(k-1)}$, $\tilde{\mathbf{C}}^{(k)}$ is the least square solution of the minimization of $f(\hat{\mathbf{A}}^{(k-1)}, \hat{\mathbf{B}}^{(k-1)}, \mathbf{C}; \mathbf{X})$ with respect to unconstrained continuous $\mathbf{C}$

$$\tilde{\mathbf{C}}^{(k)} = \arg\min_{\mathbf{C}} \left\|\mathbf{X} - \left(\hat{\mathbf{A}}^{(k-1)} \odot \hat{\mathbf{B}}^{(k-1)}\right)\mathbf{C}^T\right\|_F^2 = \left(\left(\hat{\mathbf{A}}^{(k-1)} \odot \hat{\mathbf{B}}^{(k-1)}\right)^{\dagger}\mathbf{X}\right)^T \tag{7}$$

Second step: project elements of $\tilde{\mathbf{C}}^{(k)}$, $\tilde{c}_{k,r}$, $k = 1, \ldots, K$, $r = 1, \ldots, R$, to the constraint set Ω.

$$\hat{c}_{k,r} = \mathrm{proj}_{\Omega}(\tilde{c}_{k,r}) \tag{8}$$

where $\mathrm{proj}_{\Omega}(\bullet)$ is the projection operator. According to different constraints, $\mathrm{proj}_{\Omega}(\bullet)$ denotes different operations. Taking CM constraint for example, the projection operator is

$$\mathrm{proj}_{\mathrm{CM}}(c) = c/||c||_2^2 \tag{9}$$

Then the k-th estimation of $\mathbf{C}$, denoted as $\hat{\mathbf{C}}^{(k)}$ with elements $\hat{c}_{k,r}$, is obtained. The k-th least square update of $\mathbf{A}$ is obtained by minimizing the cost function, keeping $\hat{\mathbf{B}}^{(k-1)}$ and $\hat{\mathbf{C}}^{(k)}$ fixed.

$$\hat{\mathbf{A}}^{(k)} = \arg\min_{\mathbf{A}} \left|\left|\mathbf{Y} - \left(\hat{\mathbf{B}}^{(k-1)} \odot \hat{\mathbf{C}}^{(k)}\right)\mathbf{A}^T\right|\right|_F^2 = \left(\left(\hat{\mathbf{B}}^{(k-1)} \odot \hat{\mathbf{C}}^{(k)}\right)^{\dagger}\mathbf{Y}\right)^T \tag{10}$$

Similarly, a better estimation of $\mathbf{B}$ is obtained as

$$\hat{\mathbf{B}}^{(k)} = \arg\min_{\mathbf{B}} \left|\left|\mathbf{Z} - \left(\hat{\mathbf{C}}^{(k)} \odot \hat{\mathbf{A}}^{(k)}\right)\mathbf{B}^T\right|\right|_F^2 = \left(\left(\hat{\mathbf{C}}^{(k)} \odot \hat{\mathbf{A}}^{(k)}\right)^{\dagger}\mathbf{Z}\right)^T \tag{11}$$

Continue this process until $\hat{\mathbf{A}}$, $\hat{\mathbf{B}}$ and $\hat{\mathbf{C}}$ converge. TALSP algorithm is presented in Table 1.

Table 1. TALSP algorithm.

Step 1: Initialize three mode matrices $\hat{\mathbf{A}}^{(0)}$, $\hat{\mathbf{B}}^{(0)}$, $\hat{\mathbf{C}}^{(0)}$, $k=0$;
Step 2: $k=k+1$
Step 3: According to (7)–(8), update $\mathbf{C}$ using $\mathbf{X}$, $\hat{\mathbf{A}}^{(k-1)}$, $\hat{\mathbf{B}}^{(k-1)}$;
Step 4: According to (10), update $\mathbf{A}$ using $\mathbf{Y}$, $\hat{\mathbf{B}}^{(k-1)}$, $\hat{\mathbf{C}}^{(k)}$;
Step 5: According to (11), update $\mathbf{B}$ using $\mathbf{Z}$, $\hat{\mathbf{C}}^{(k)}$, $\hat{\mathbf{A}}^{(k)}$;
Step 6: repeat steps 2–5. Define a fitting error variable $\varepsilon = \|\mathbf{X} - \left(\hat{\mathbf{A}}^{(k-1)} \odot \hat{\mathbf{B}}^{(k-1)}\right) \mathbf{C}^{(k-1)^T}\|_F^2 - \|\mathbf{X} - \left(\hat{\mathbf{A}}^{(k)} \odot \hat{\mathbf{B}}^{(k)}\right) \mathbf{C}^{(k)^T}\|_F^2$
When ε becomes very small (less than10^{-8}), algorithm is finished.

3.2. TALSSIC Algorithm

A limitation of TALSP is that the projection procedure in **C**-update breaks its monotone convergence, which means that TALSP algorithm cannot guarantee to decrease or hold the value of cost function in each matrix updating procedure[†]. TALSSIC is also a nonlinear alternating iterative algorithm. However, it is most important that TALSSIC can be guaranteed to monotonically converge to the constrained least square solution.

The main difference between TALSSIC and TALSP is the update procedure of mode matrix **C**. TALSSIC exploits successive interference cancelation strategy to update **C** in column wise. Assume that $\hat{\mathbf{A}}^{(k)}$, $\hat{\mathbf{B}}^{(k)}$, $\hat{\mathbf{C}}^{(k)}$ stand for the k-th updates of **A**, **B**, and **C**, respectively. Define $\hat{\mathbf{H}}^{(k)} = \hat{\mathbf{A}}^{(k)} \odot \hat{\mathbf{B}}^{(k)}$. $\hat{\mathbf{a}}_r^{(k)}$, $\hat{\mathbf{b}}_r^{(k)}$, $\hat{\mathbf{c}}_r^{(k)}$, $\hat{\mathbf{h}}_r^{(k)}$ are columns of $\hat{\mathbf{A}}^{(k)}$, $\hat{\mathbf{B}}^{(k)}$, $\hat{\mathbf{C}}^{(k)}$, $\hat{\mathbf{H}}^{(k)}$. Consider (7) in column wise during the $(k-1)$-th iteration:

$$\mathbf{X} = \left(\hat{\mathbf{A}}^{(k-1)} \odot \hat{\mathbf{B}}^{(k-1)}\right) \hat{\mathbf{C}}^{(k-1)^T} + \mathbf{E}_X = \mathbf{H}^{(k-1)} \mathbf{C}^{(k-1)^T} + \mathbf{E}_X$$

$$= \mathbf{h}_1^{(k-1)} \mathbf{c}_1^{(k-1)^T} + \sum_{r=2}^{R} \mathbf{h}_r^{(k-1)} \mathbf{c}_r^{(k-1)^T} + \mathbf{E}_X = \mathbf{h}_1^{(k-1)} \mathbf{c}_1^{(k-1)^T} + \mathbf{X}_1 + \mathbf{E}_1 \quad (12)$$

where $\mathbf{X}_1 = \sum_{r=2}^{R} \mathbf{h}_r^{(k-1)} \mathbf{c}_r^{(k-1)^T}$. $\mathbf{E}_1$ is the additive noise during the

[†] Although we have found that TALSP is monotonically convergent mostly, a strictly demonstration is failed.

update of $\mathbf{c}_1$. The unconstrained least square solution of $\mathbf{c}_1$ is

$$\tilde{\mathbf{c}}_1^{(k)} = \arg\min_{\mathbf{c}_1} \left|\left|\mathbf{X} - \mathbf{h}_1^{(k-1)}\mathbf{c}_1^T - \mathbf{X}_1\right|\right|_F^2 = \left(\frac{\left(\mathbf{h}_1^{(k-1)}\right)^H}{\left|\left|\mathbf{h}_1^{(k-1)}\right|\right|_2^2}\left(\mathbf{X} - \mathbf{X}_1\right)\right)^T \tag{13}$$

Project the elements of $\tilde{\mathbf{c}}_1^{(k)}$ to constraint set Ω

$$\hat{\mathbf{c}}_1^{(k)} = \mathrm{proj}_\Omega\left(\tilde{\mathbf{c}}_1^{(k)}\right) \tag{14}$$

where $\hat{\mathbf{c}}_1^{(k)}$ is the estimation of $\mathbf{c}_1$ in the k-th iteration. Then update $\hat{\mathbf{c}}_1^{(k)}$ to $\hat{\mathbf{C}}^{(k-1)}$ (replace $\hat{\mathbf{c}}_1^{(k-1)}$ with $\hat{\mathbf{c}}_1^{(k)}$) and continue to update $\mathbf{c}_r$, $r = 2, \ldots, R$. Without loss of generality, we give the update procedure of $\mathbf{c}_r$. Define matrix $\mathbf{X}_r$

$$\mathbf{X}_r = \sum_{i=1}^{r-1} \hat{\mathbf{h}}_i^{(k-1)}\hat{\mathbf{c}}_i^{(k)^T} + \sum_{i=r+1}^{R} \hat{\mathbf{h}}_i^{(k-1)}\hat{\mathbf{c}}_i^{(k-1)^T} \tag{15}$$

The formulation of $\mathbf{X}$ in the rth update is

$$\mathbf{X} = \hat{\mathbf{h}}_r^{(k-1)}\hat{\mathbf{c}}_r^{(k-1)^T} + \mathbf{X}_r + \mathbf{E}_r \tag{16}$$

where $\mathbf{E}_r$ is the additive noise during $\mathbf{c}_r$-update. $\hat{\mathbf{c}}_r^{(k)}$ can be obtained as follow

$$\hat{\mathbf{c}}_r^{(k)} = \mathrm{proj}_\Omega\left(\frac{\left(\hat{\mathbf{h}}_r^{(k-1)}\right)^H}{\left|\left|\hat{\mathbf{h}}_r^{(k-1)}\right|\right|_r^2}\left(\mathbf{X} - \mathbf{X}_r\right)\right)^T \tag{17}$$

$\hat{\mathbf{C}}^{(k)}$ is then obtained when all columns of $\mathbf{C}$ are updated. The update procedures of $\mathbf{A}$ and $\mathbf{B}$ are the same as TALSP algorithm. TALSSIC algorithm is concluded in Table 2.

3.3. Convergence

Unlike TALSP algorithm, TALSSIC algorithm is monotonically convergent. Here we give a simple demonstration, which is equivalent to show that matrices update procedures of TALSSIC only decrease or hold, but never increase the value of the cost function. The updates of $\mathbf{A}$ and $\mathbf{B}$ are standard least square procedures. Then the following inequalities are always hold

$$f\left(\mathbf{A}^{(k)}, \mathbf{B}, \mathbf{C}; \mathbf{X}\right) \leq f\left(\mathbf{A}^{(k-1)}, \mathbf{B}, \mathbf{C}; \mathbf{X}\right) \tag{18}$$

$$f\left(\mathbf{A}, \mathbf{B}^{(k)}, \mathbf{C}; \mathbf{X}\right) \leq f\left(\mathbf{A}, \mathbf{B}^{(k-1)}, \mathbf{C}; \mathbf{X}\right) \tag{19}$$

Table 2. TALSSIC algorithm.

Step 1: Initialize three mode matrices $\hat{\mathbf{A}}^{(0)}$, $\hat{\mathbf{B}}^{(0)}$, $\hat{\mathbf{C}}^{(0)}$, $k=0$;
Step 2: $k=k+1$
Step 3: According to (12)–(17), update $\mathbf{C}$ using $\mathbf{X}$, $\hat{\mathbf{A}}^{(k-1)}$, $\hat{\mathbf{B}}^{(k-1)}$;
Step 4: According to (10), update $\mathbf{A}$ using $\mathbf{Y}$, $\hat{\mathbf{B}}^{(k-1)}$, $\hat{\mathbf{C}}^{(k)}$;
Step 5: According to (11), update $\mathbf{B}$ using $\mathbf{Z}$, $\hat{\mathbf{C}}^{(k)}$, $\hat{\mathbf{A}}^{(k)}$;
Step 6: repeat steps 2–5. Define a fitting error variable $\varepsilon = \|\|\mathbf{X} - \left(\hat{\mathbf{A}}^{(k-1)} \odot \hat{\mathbf{B}}^{(k-1)}\right)\mathbf{C}^{(k-1)^T}\|\|_F^2 - \|\|\mathbf{X} - \left(\hat{\mathbf{A}}^{(k)} \odot \hat{\mathbf{B}}^{(k)}\right)\mathbf{C}^{(k)^T}\|\|_F^2$
When ε becomes very small (less than 10^{-8}), algorithm is finished.

Therefore, if

$$f\left(\mathbf{A},\mathbf{B},\mathbf{C}^{(k)};\mathbf{X}\right) \le f\left(\mathbf{A},\mathbf{B},\mathbf{C}^{(k-1)};\mathbf{X}\right) \tag{20}$$

is satisfied, TALSSIC algorithm can be demonstrated monotonically convergent. Now we prove the validity of (20). Consider the following constrained least square problem:

$$\hat{\mathbf{c}} = \arg\min_{\mathbf{c}\in\Omega} \left|\left|\mathbf{X} - \mathbf{h}\mathbf{c}^T\right|\right|_F^2 \tag{21}$$

[35] has pointed out that (21) is equivalent to two procedures:

$$\tilde{\mathbf{c}} = \arg\min \left|\left|\mathbf{X} - \mathbf{h}\mathbf{c}^T\right|\right|_F^2 \tag{22}$$

$$\hat{\mathbf{c}} = \arg\min_{\mathbf{c}\in\Omega} \left|\left|\tilde{\mathbf{c}} - \mathbf{c}\right|\right|_F^2 \tag{23}$$

where $\tilde{\mathbf{c}}$ is the unconstrained least square solution of (21). Therefore, (17) is the constrained least square solution of (16), and the following inequality is always satisfied

$$\begin{aligned} &\left|\left|\mathbf{X} - \mathbf{X}_r - \mathbf{h}_r\hat{\mathbf{c}}_r^{(k)^T}\right|\right|_F^2 \\ &= \min_{c_r} \left|\left|\mathbf{X} - \mathbf{X}_r - \mathbf{h}_r\mathbf{c}_r^T\right|\right|_F^2 \le \left|\left|\mathbf{X} - \mathbf{X}_r - \mathbf{h}_r\hat{\mathbf{c}}_r^{(k-1)^T}\right|\right|_F^2 \end{aligned} \tag{24}$$

Then it follows

$$\begin{aligned} &f\left(\mathbf{A},\mathbf{B},\mathbf{C}^{(k)};\mathbf{X}\right) \\ &= \left|\left|\mathbf{X} - (\mathbf{A}\odot\mathbf{B})\mathbf{C}^{(k)^T}\right|\right|_F^2 = \left|\left|\mathbf{X} - \mathbf{H}\mathbf{C}^{(k)^T}\right|\right|_F^2 = \left|\left|\mathbf{X} - \sum_{r=1}^{R}\mathbf{h}_r\hat{\mathbf{c}}_r^{(k)^T}\right|\right|_F^2 \end{aligned}$$

$$
\begin{aligned}
&= \left|\left|\mathbf{X} - \mathbf{X}_{R-1} - \mathbf{h}_R \hat{\mathbf{c}}_R^{(k)^T}\right|\right|_F^2 = \min_{\mathbf{c}} \left|\left|\mathbf{X} - \mathbf{X}_{R-1} - \mathbf{h}_R \mathbf{c}^T\right|\right|_F^2 \\
&\leq \left|\left|\mathbf{X} - \mathbf{X}_{R-1} - \mathbf{h}_R \hat{\mathbf{c}}_R^{(k-1)^T}\right|\right|_F^2 = \left|\left|\mathbf{X} - \mathbf{X}_{R-2} - \mathbf{h}_{R-1} \hat{\mathbf{c}}_{R-1}^{(k)^T}\right|\right|_F^2 \\
&= \min_{\mathbf{c}} \left|\left|\mathbf{X} - \mathbf{X}_{R-2} - \mathbf{h}_{R-1} \mathbf{c}^T\right|\right|_F^2 \leq \left|\left|\mathbf{X} - \mathbf{X}_{R-2} - \mathbf{h}_{R-1} \hat{\mathbf{c}}_{R-1}^{(k-1)^T}\right|\right|_F^2 \\
&\vdots \\
&\leq \left|\left|\mathbf{X} - \mathbf{X}_1 - \mathbf{h}_1 \hat{\mathbf{c}}_1^{(k-1)^T}\right|\right|_F^2 = \left|\left|\mathbf{X} - \sum_{r=1}^{R} \mathbf{h}_r \hat{\mathbf{c}}_r^{(k-1)^T}\right|\right|_F^2 \\
&= \left|\left|\mathbf{X} - \mathbf{H}\mathbf{C}^{(k-1)^T}\right|\right|_F^2 = \left|\left|\mathbf{X} - (\mathbf{A} \odot \mathbf{B})\mathbf{C}^{(k-1)^T}\right|\right|_F^2 \\
&= f(\mathbf{A}, \mathbf{B}, \mathbf{C}^{(k-1)}; \mathbf{X}) \qquad (25)
\end{aligned}
$$

The proof of (20) is finished. According to (18) $\sim$ (20), TALSSIC algorithm is demonstrated monotonically convergent.

3.4. Complexity and Initialization

In the **C**-update procedure of algorithms, the multiplication cost of TALSP is $IJR^2 + IJKR$ while the complexity of TALSSIC is $3IJR + IJR^2 + IJKR$. Note that TALSSIC algorithm has higher computation complexity than TALSP algorithm. However, because of the similarity of these two algorithms, we can use TALSP to 'initialize' TALSSIC to ensure convergence and decrease complexity during signal processing. The main procedure can be summarized as two steps: TALSP is firstly used to pre-fit the triple data (e.g., the receiving signals of sensor array). When TALSP worsens the fit or the fitting error variable ε is relatively small (less than 1e-4, for example) in the $(k+1)$th iteration, then we use the estimations $\mathbf{A}^{(k)}$, $\mathbf{B}^{(k)}$ and $\mathbf{C}^{(k)}$, obtained from TALSP, to initialize TALSSIC and continue to fit the data until algorithm converges. This method combines the advantage of TALSP (low computation costs) and the benefits of TALSSIC (monotone convergence). In the following simulations, we use this initialization method to evaluate the performance of proposed algorithms.

4. SIMULATION RESULTS

In this section, we apply constrained PARAFAC decomposition to model multiple invariance sensor array signals and accomplish joint azimuth and elevation angles estimation by using TALSSIC algorithm.

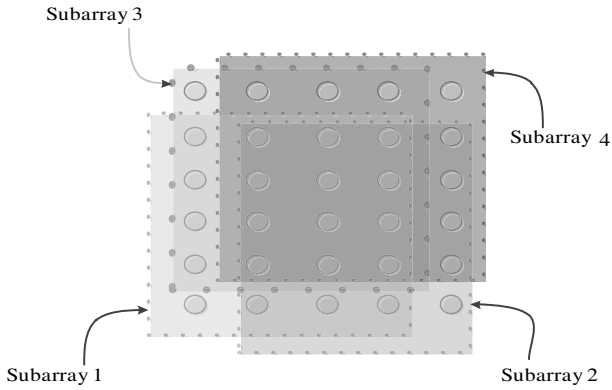

Figure 2. The arrangement of 6×5 rectangular array and subarraies.

The following four simulations will illustrate the improvements of the proposed constrained model and algorithms listed in Section 1. Firstly, simulations 1 and 2 evaluate the performance of parameters estimation of the TALSSIC-based algorithm in the forms of both scatter diagram and mean squared error curve, compared with TALS-based algorithm and traditional ESPRIT algorithm. Secondly, simulation 3 depicts the convergence performance of the proposed algorithms. Finally, simulation 4 gives the performance of TALSSIC-based and TALS-based algorithms when correlated factors are involved in the data model.

As discussed in Section 3, TALSP algorithm is used to initialize TALSSIC. Consider a 6×5 rectangular array and four subarraies, depicted in Figure 2 [9, 36].

Assume that the baseband signals are modulated as QPSK with CM structure. The received signal of multiple invariance sensor array can be formed as constrained PARAFAC model.

$$\mathbf{X} = (\mathbf{\Phi} \odot \mathbf{A})\, \mathbf{S}^T + \mathbf{E}, \quad \mathbf{S} \in \Omega \tag{26}$$

Three mode matrices are the subarray response matrix $\mathbf{A}$, parameters matrix $\mathbf{\Phi}$, and baseband signal matrix $\mathbf{S}$, formulated as

$$\mathbf{A} = [\mathbf{a}_1, \ldots, \mathbf{a}_R] = \begin{bmatrix} 1 & \ldots & 1 \\ e^{-j\frac{2\pi d}{\lambda}\sin(\theta_1)} & \ldots & e^{-j\frac{2\pi d}{\lambda}\sin(\theta_R)} \\ \vdots & \vdots & \vdots \\ e^{-j\frac{2\pi (I-1) d}{\lambda}\sin(\theta_1)} & \ldots & e^{-j\frac{2\pi (I-1) d}{\lambda}\sin(\theta_R)} \end{bmatrix}$$

$$\mathbf{\Phi}=\begin{bmatrix} 1 & \cdots & 1 \\ e^{-j\frac{2\pi d}{\lambda}\sin(\theta_1)} & \cdots & e^{-j\frac{2\pi d}{\lambda}\sin(\theta_R)} \\ e^{-j\frac{2\pi d}{\lambda}\cos(\theta_1)\sin(\phi_1)} & \cdots & e^{-j\frac{2\pi d}{\lambda}\cos(\theta_R)\sin(\phi_R)} \\ e^{-j\frac{2\pi d}{\lambda}(\sin(\theta_1)+\cos(\theta_1)\sin(\phi_1))} & \cdots & e^{-j\frac{2\pi d}{\lambda}(\sin(\theta_R)+\cos(\theta_R)\sin(\phi_R))} \end{bmatrix} \quad (27)$$

$$\mathbf{S}=\begin{bmatrix} s_{11}, & s_{12} & \ldots, & s_{1R} \\ s_{21}, & s_{22} & \ldots, & s_{2R} \\ \vdots & \vdots & \vdots & \\ s_{K1}, & s_{K2} & \ldots, & s_{KR} \end{bmatrix}$$

where θ, ϕ denote azimuth and elevation. λ is the wavelength of signals. d is the distance between adjacent antenna. R is the number of sources. K denotes the length of data block and is assumed to be 100 in the following simulations. I is the length of subarray. According to Figure 2, I is equal to 5. Parameters, including azimuth and elevation, are involved in $\mathbf{\Phi}$. The TALS-based algorithm [9] and traditional ESPRIT algorithm [36] are also simulated just for comparison. SNR is defined in terms of the noisy data model (26)

$$\mathrm{SNR} = 10\log_{10}\frac{\left|\left|\bar{\mathbf{X}}\right|\right|_F^2}{||\mathbf{E}||_F^2} \quad (28)$$

Three sources are considered in the simulation. The azimuths and elevations are listed in Table 3.

4.1. Simulation 1

The performance of azimuth and elevation estimations of TALSSIC-based algorithm, TALS-based algorithm and ESPRIT algorithm are evaluated in this simulation. CM constraint is involved in TALSSIC-based algorithm. SNR is 40 dB, and 100 independent Monte Carlo runs are used to evaluate performance. Figures 3–5 depict the azimuth-elevation scatter diagrams of three algorithms. The X coordinate stands for azimuth, and Y coordinate stands for elevation. The left sub-figure of each figure depicts the estimated azimuth-elevation diagrams of all 3 waves, and the right two sub-figures, titled as (a)

Table 3. Azimuths and elevations of sources.

	Azimuth (θ)	Elevation (ϕ)
source 1	5°	10°
source 2	10°	15°
source 3	15°	20°

and (b), are the zoom-in diagrams of two waves with parameters (5°, 10°) and (10°, 15°). It is illustrated that the proposed TALSSIC-based algorithm has a better performance than TALS-based algorithm and ESPRIT algorithm.

4.2. Simulation 2

This simulation evaluates the root mean squared error (RMSE) performance of the three algorithms in parameter estimation. Since matrix $\mathbf{\Phi}$ involves the full information of the azimuth and elevation,

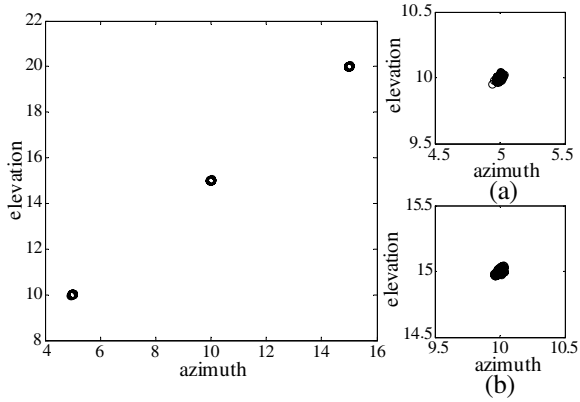

Figure 3. Azimuth-elevation scatter diagram of TALSSIC-based algorithm.

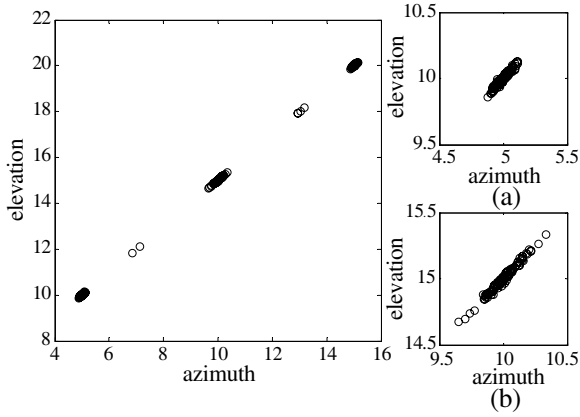

Figure 4. Azimuth-elevation scatter diagram of TALS-based algorithm.

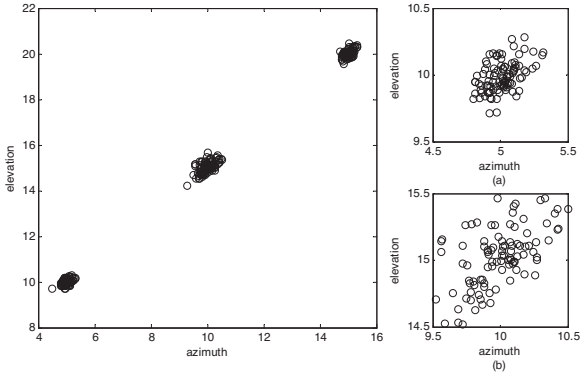

Figure 5. Azimuth-elevation scatter diagram of ESPRIT algorithm.

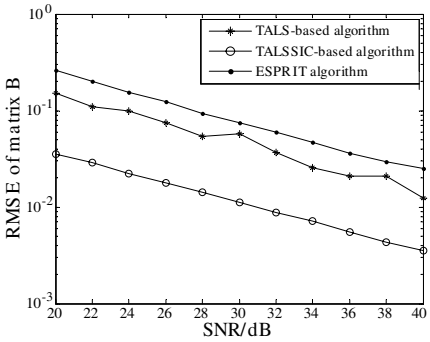

Figure 6. RMSE curve of parameter estimation versus SNR.

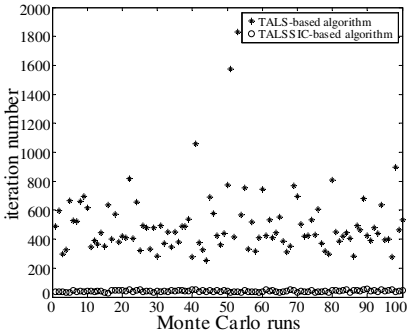

Figure 7. Iteration number in 100 Monte Carlo runs (SNR = 20 dB).

we calculate the RMSE between the estimated $\hat{\mathbf{\Phi}}$ and the original $\mathbf{\Phi}$ to evaluate the RMSE performance of parameters estimation, formulated as the Frobenius norm of $(\mathbf{\Phi} - \hat{\mathbf{\Phi}}_i)$

$$\xi = \frac{1}{Q} \sum_{i=1}^{Q} \left|\left| \mathbf{\Phi} - \hat{\mathbf{\Phi}}_i \right|\right|_F \tag{29}$$

where $\hat{\mathbf{\Phi}}_i$ is the estimated parameter matrix in the ith simulation and Q the number of independent runs. SNR varies from 20 dB to 40 dB. 100 independent Monte Carlo runs are simulated. Figure 6 plots the RMSE curve versus SNR in logarithmic coordinates. It is depicted that the RMSE values of the proposed TALSSIC-based algorithm are less than the other two algorithms under either high or low SNR conditions.

The results of simulations 1 and 2 show that TALSSIC-based

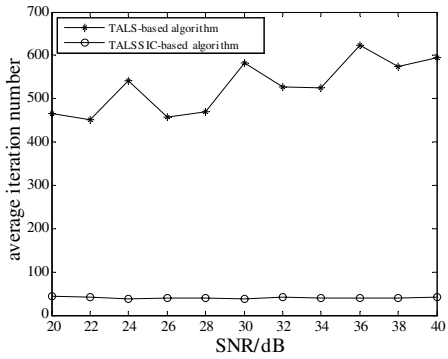

Figure 8. Average iteration number curve versus SNR.

algorithm has better accuracy of parameter estimation than TALS-based algorithm and ESPRIT algorithm, because TALSSIC-based algorithm not only makes use of three diversities of trilinear data model, but also exploits the structure of signals to improve the performance of parameter estimation.

4.3. Simulation 3

The convergence performance of constrained and unconstrained algorithms is evaluated in this simulation. Figure 7 depicts the iteration number of TALS-based algorithm and TALSSIC-based algorithm in 100 independent runs when SNR is 20 dB. Figure 8 depicts the average iteration number curve of two algorithms versus SNR. Obviously, TALSSIC-based algorithm converges faster than TALS-based algorithm, which illustrates that the structure reconstruction during matrix update procedure can improve the convergence speed. Note that the complexity of an iterative algorithm is related to its convergence speed and the computation cost of each iteration. The simulation results also imply that TALSSIC needs lower computation complexity than TALS in array signal processing.

4.4. Simulation 4

As mentioned in Section 1, correlated factors in mode matrix may lead to performance loss in trilinear decomposition. This simulation will evaluate the performance of algorithms when correlated factors are involved in subarray matrix $\mathbf{A}$. Due to (27), the correlation property of factors in $\mathbf{A}$ can be characterized by the similarity of $\theta_1, \ldots, \theta_R$. To simplify the calculation, we change the azimuth of source 1, denoted as

θ_1, from 5° to 9.9° and keep azimuth of source 2 and source 3 constant, as $\theta_2 = 10°$, $\theta_3 = 15°$. The correlation degree of factors $\mathbf{a}_1$ and $\mathbf{a}_2$, denoted as $\rho_{1,2}$, can be characterized by the inverse of their Edices distance.

$$\rho_{1,2} = \frac{1}{\sqrt{(\mathbf{a}_1 - \mathbf{a}_2)^H (\mathbf{a}_1 - \mathbf{a}_2)}} \tag{30}$$

Assume that SNR is 40 dB. Table 4 presents the azimuths of three sources and the related $\rho_{1,2}$.

$\rho_{1,2}$ is increased when θ_1 and θ_2 become closer and closer. Figure 9 presents the RMSE curve of parameter estimation versus $\rho_{1,2}$ while Figure 10 depicts the average iteration number curve versus $\rho_{1,2}$.

The simulation results illustrate that the performances of both parameter estimation and convergence of TALS-based algorithm are decreased sharply as $\rho_{1,2}$ increased, which implies that TALS-based algorithm is not suitable for data with correlated factors. However,

Table 4. Azimuths of three sources and the related $\rho_{1,2}$.

θ_1	θ_2	θ_3	$\rho_{1,2}$
5°	10°	15°	0.69
6°	10°	15°	0.86
7°	10°	15°	1.13
8	10°	15°	1.7
9	10°	15°	3.38
9.5°	10°	15°	6.75
9.9°	10°	15°	33.8

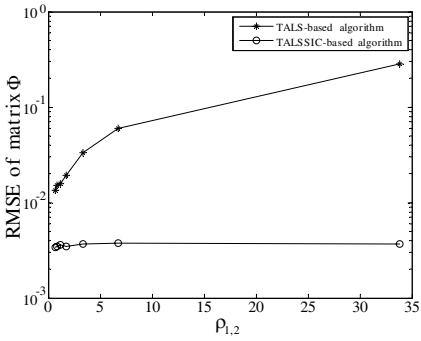

Figure 9. RMSE curve of parameter estimation versus $\rho_{1,2}$.

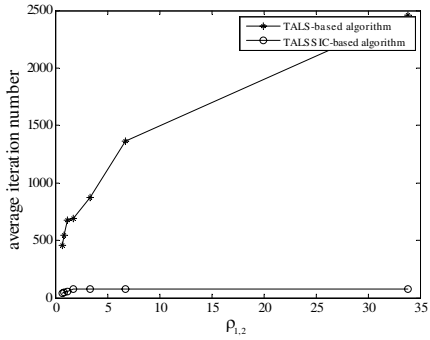

Figure 10. Average iteration number curve versus $\rho_{1,2}$.

TALSSIC-based algorithm still performs very well in either low or high $\rho_{1,2}$ conditions. In array signal processing aspect, high correlated factors are often caused by coherent signals in multipath transmitting and radar receiving scenarios. It can be concluded that TALSSIC-based algorithm is still valid in these applications.

5. CONCLUSION

This paper exploits structure constraint in trilinear decomposition and links it to array signal processing. Constrained PARAFAC model is introduced for model analysis. Two new algorithms, named TALSP and TALSSIC, are proposed to accomplish constrained PARAFAC decomposition in signal processing. We apply the proposed model and algorithms to azimuth and elevation estimation of multiple invariance sensor arrays. Simulations show that TALSSIC-based algorithm outperforms traditional TALS-based algorithm and ESPRIT algorithm in terms of the performance of both parameter estimation and convergence. Especially, the proposed algorithms can still work well even if high correlated columns are involved in the data model, which may be encountered in multipath transmitting and radar receiving scenarios.

ACKNOWLEDGMENT

This work is supported by China NSF Grants (61101104, 61071090, 61100195), National Science and Technology Major Project (2011ZX03005-004-03), Jiangsu "973" Project (BK2011027), a project funded by the Priority Academic Program Development of Jiangsu Higher Education Institutions-Information and Communication Engineering; Nanjing University of Posts & Telecommunications Project (NY211010). The authors wish to thank the anonymous reviewers for their valuable suggestions on improving this paper.

REFERENCES

1. Krim, H. and M. Viberg, "Two decades of array signal processing research: the parametric approach," *IEEE Signal Processing Magazine*, Vol. 13, No. 4, 67–94, 1996.
2. Zhang, X., X. Gao, and W. Chen, "Improved blind 2D-direction of arrival estimation with L-shaped array using shift invariance property," *Journal of Electromagnetic Waves and Applications*, Vol. 23, Nos. 5–6, 593–606, 2009.

3. Liang, J. and D. Liu, "Two L-Shaped array-based 2-D DOAs estimation in the presence of mutual coupling," *Progress In Electromagnetics Research*, Vol. 112, 273–298, 2011.
4. Liang, J., D. Liu, X. Zeng, W. Wang, J. Zhang, and H. Chen, "Joint azimuth-elevation/(-range) estimation of mixed near-field and far-field sources using two-stage separated steering vector-based algorithm," *Progress In Electromagnetics Research*, Vol. 113, 17–46, 2011.
5. Mallipeddi, R., J. P. Lie, P. N. Suganthan, S. G. Razul, and C. M. S. See, "A differential evolution approach for robust adaptive beamforming based on joint estimation of look direction and array geometry," *Progress In Electromagnetics Research*, Vol. 119, 381–394, 2011.
6. Yang, P., F. Yang, and Z.-P. Nie, "DOA estimation with sub-array divided technique and interpolated ESPRIT algorithm on a cylindrical conformal array antenna," *Progress In Electromagnetics Research*, Vol. 103, 201–216, 2010.
7. Lee, J.-H., Y.-S. Jeong, S.-W. Cho, W.-Y. Yeo, and K. S. J. Pister, "Application of the newton method to improve the accuracy of TOA estimation with the beamforming algorithm and the MUSIC algorithm," *Progress In Electromagnetics Research*, Vol. 116, 475–515, 2011.
8. Zaharis, Z. D. and T. V. Yioultsis, "A novel adaptive beamforming technique applied on linear antenna arrays using adaptive mutated boolean PSO," *Progress In Electromagnetics Research*, Vol. 117, 165–179, 2011.
9. Sidiropoulos, N. D., R. Bro, and G. B. Giannakis, "Parallel factor analysis in sensor array processing," *IEEE Transactions on Signal Processing*, Vol. 48, No. 8, 2377—2388, 2000.
10. Zhang, X., X. Gao, and Z. Wang, "Blind PARALIND multiuser detection for smart antenna CDMA system over multipath fading channel," *Progress In Electromagnetics Research*, Vol. 89, 23–38, 2009.
11. Zhang, X., D. Wang, and D. Xu, "Novel blind joint direction of arrival and frequency estimation for uniform linear array," *Progress In Electromagnetics Research*, Vol. 86, 199–215, 2008.
12. Kruskal, J. B., "Three-way arrays: Rank and uniqueness of trilinear decompositions, with application to arithmetic complexity and statistics," *Linear Algebra Applicat.*, Vol. 18, 95–138, 1977.
13. Sidiropoulos, N. D., G. B. Giannakis, and R. Bro, "Blind PARAFAC receivers for DS-CDMA systems," *IEEE Transactions*

on Signal Processing, Vol. 48, No. 3, 810–823, 2000.

14. Zhang, X. and D. Xu, "Deterministic blind beamforming for electromagnetic vector sensor array," *Progress In Electromagnetics Research*, Vol. 84, 363–377, 2008.
15. Liu, X. and N. D. Sidiropoulos, "Parafac methods for blind beamforming: Multilinear ALS performance and CRB," *IEEE International Conference on Acoustics, Speech, and Signal Processing*, Vol. 5, 3128–3131, 2000.
16. Shi, Y. and X. Zhang, "Quadrilinear decomposition-based blind signal detection for polarization sensitive uniform square array," *Progress In Electromagnetics Research*, Vol. 87, 263–278, 2008.
17. Zhang, X., D. Wang, and D. Xu, "Novel blind joint direction of arrival and polarization estimation for polarization-sensitive uniform circular array," *Progress In Electromagnetics Research*, Vol. 86, 19–37, 2008.
18. Gong X. F., Z. W. Liu, and Y. G. Xu, "Regularised parallel factor analysis for the estimation of direction-of-arrival and polarisation with a single electromagnetic vector-sensor," *IET Signal Processing*, Vol. 5, No. 4, 390–396, 2011.
19. Zhang, X., Z. Xu, L. Xu, and D. Xu, "Trilinear decomposition-based transmit angle and receive angle estimation for multiple-input multiple-output radar," *IET Radar, Sonar & Navigation*, Vol. 5, No. 6, 626–631, 2011.
20. Nion, D. and N. D. Sidiropoulos, "Adaptive algorithms to track the PARAFAC decomposition of a third-order tensor," *IEEE Transactions on Signal Processing*, Vol. 57, No. 6, 2299–2310, 2009.
21. Tomasi, G. and R. Bro, "A comparison of algorithms for fitting the PARAFAC model," *Computational Statistics & Data Analysis*, Vol. 50, 1700–1734, 2006.
22. Sergiy, A., R. Yue, N. D. Sidiropoulos, and A. B. Gershman, "Robust iterative fitting of multilinear models," *IEEE Transactions on Signal Processing*, Vol. 53, No. 8, 2678–2689, 2005.
23. Li, W.-X., Y.-P. Li, and W.-H. Yu, "On adaptive beamforming for coherent interference suppression via virtual antenna array," *Progress In Electromagnetics Research*, Vol. 125, 165–184, 2012.
24. Park, G. M., H. G. Lee, and S. Y. Hong, "DOA resolution enhancement of coherent signals via spatial averaging of virtually expanded arrays," *Journal of Electromagnetic Waves and Applications*, Vol. 24, No. 1, 61–70, 2010.

25. Zhang, X., J. Yu, G. Feng, and D. Xu, "Blind direction of arrival estimation of coherent sources using multi-invariance property," *Progress In Electromagnetics Research*, Vol. 88, 181–195, 2008
26. Bro, R. and C. A. Anderddon, "Improving the speed of multiway algorithms Part II: Compression," *Chemometrics and Intelligent Laboratory Systems*, Vol. 42, 105–113, 1998.
27. Bro, R., "Multi-way analysis in the food industry: Models, algorithms, and applications," Ph.D. Thesis, University of Amsterdam, Amsterdam, 1998.
28. Rajih, M., P. Comon, and R. A. Harshman, "Enhanced line search: A novel method to accelerate PARAFAC," *SIAM Journal on Matrix Analysis and Applications*, Vol. 30, No. 3, 1128–1147, 2008.
29. Nion, D. and L. D. Lathauwer, "An enhanced line search scheme for complex-valued tensor decompositions application in DS-CDMA," *Signal Processing*, Vol. 88, 749–755, 2008.
30. Bro, R., "PARAFAC. Tutorial and applications," *Chemometrics and Intelligent Laboratory Systems*, Vol. 38, 149–171, 1997.
31. Bro, R., R. A. Harshman, N. D. Sidiropoulos, et al., "Modeling multi-way data with linearly dependent loadings," *Journal of Chemometrics*, Vol. 23, No. 7–8, 324–340, 2009.
32. Richard, A. H. and E. L. Margaret, "PARAFAC: Parallel factor analysis," *Computational Statistics & Data Analysis*, Vol. 18, 39–72, 1994.
33. Van der Veen, A. J., S. Talwar, A. Paulraj, "Blind identification of FIR channels carrying multiple finite alphabet signals," *International Conference on Acoustics, Speech, and Signal Processing*, Vol. 2, 1213–1216, 1995.
34. Manioudakis, S., "Blind estimation of space-time coded systems using the finite alphabet-constant modulus algorithm," *IEE Proc. — Vis. Image Signal Process.*, Vol. 153, No. 5, 549–556, 2006.
35. Bro, R. and N. D. Sidropoulos, "Least squares algorithms under unimodality and nonnegativity constraints," *J. Chemometr.*, Vol. 12, 223–247, 1998.
36. Swindlehurst, A. and T. Kailath, "Algorithms for azimuth-elevation direction finding using regular array geometries," *IEEE Transactions on Aerospace and Electronic Systems*, Vol. 29, No. 1, 145–156, 1993.